

**Fluorous-Phase Ion-Selective pH Electrodes:
Electrode Body and Ionophore Optimization for Measurements in
the Physiological pH Range**

Xin V. Chen, Maral P.S. Mousavi,¹ and Philippe Bühlmann*

Department of Chemistry, University of Minnesota, 207 Pleasant St. SE, Minneapolis, MN 55455, United States

* buhlmann@umn.edu

¹ Current address: Dept. Biomedical Engineering, University of Southern California, 1042 Downey Way, Los Angeles CA 90089

Abstract

Because of their low polarity and polarizability, fluorous sensing membranes are both hydrophobic and lipophobic and exhibit very high ion selectivities. Here, we report on a new fluorous-membrane ion-selective electrode (ISE) with a wide sensing range centered around physiologically relevant pH values. The fluorophilic tris[perfluoro(octyl)butyl]amine ($\text{N}[(\text{CH}_2)_4\text{R}_{f8}]_3$) was synthesized and tested as a new H^+ ionophore using a redesigned electrode body that provides excellent mechanical sealing and much improved measurement reliability. In a challenging 1 M KCl background, these fluorous-phase ISEs exhibit a sensing range from pH 2.2 to 11.2, which is one of the widest working ranges reported to date for ionophore-based H^+ ISEs. High selectivities against common interfering ions such as K^+ , Na^+ , and Ca^{2+} were determined (selectivity coefficients: $\log K_{\text{H},\text{K}}^{\text{pot}} = -11.6$; $\log K_{\text{H},\text{Na}}^{\text{pot}} = -12.4$; $\log K_{\text{H},\text{Ca}}^{\text{pot}} < -10.2$). Use of the $\text{N}[(\text{CH}_2)_4\text{R}_{f8}]_3$ ionophore with its $-(\text{CH}_2)_4-$ spacers separating the amino group from the strongly electron-withdrawing perfluorooctyl groups improved the potentiometric selectivity as compared to the less basic tris[perfluoro(octyl)propyl]amine ionophore. Use of $\text{N}[(\text{CH}_2)_4\text{R}_{f8}]_3$ also made the ISE less prone to counter anion failure (i.e., Donnan failure) at low pH than use of tris[perfluoro(octyl)pentyl]amine with its longer $-(\text{CH}_2)_5-$ spacers, which more effectively shield the amino center from the perfluorooctyl groups. In addition, we exposed both conventional plasticized PVC-phase pH ISEs and fluorous-phase pH ISEs to 10% serum for five days. Results show that the PVC-phase ISEs lost selectivity while their fluorous-phase counterparts did not.

Ionophore-based ion-selective electrodes (ISEs) have been well-established analytical tools for more than four decades and have applications in many fields, including clinical diagnostics, environmental analysis, and industry process control.¹⁻⁸ Recent advancements have focused on improving their detection limits,⁹⁻¹⁴ developing calibration-free ISEs,¹⁵⁻¹⁷ making them suitable for new applications,¹⁸⁻²⁰ and expanding sensing ranges.²¹⁻²² The latter are defined by the difference between their upper and lower detection limits, which are determined by the co-extraction of counter ions (also known as Donnan failure)²³⁻²⁸ and the interference from ions other than the target ion,²⁹ respectively.

Our group previously reported the development of fluorous-phase ISEs, i.e., ISEs with highly fluorinated sensing membrane matrixes that are both highly hydrophobic and highly lipophobic. The extremely low polarity and polarizability of fluorous phases³⁰⁻³¹ significantly suppress the non-specific phase transfer of both counter-ions and interfering ions into such sensing membranes, thereby expanding the upper and lower detection limits. The introduction of a fluorophilic tetraphenylborate derivative enabled the very first fluorous-phase ion exchanger electrodes.²¹ The use of fluorophilic ionophores subsequently permitted the development of fluorous-phase ISEs for Ag^+ , H^+ , and CO_3^{2-} .^{14, 28, 32} Self-supporting fluorous membranes for ISEs were demonstrated using the amorphous perfluoropolymer Teflon AF and semifluorinated polymers,³³⁻³⁴ and the use of fluorous-phase ISEs was shown for biological and environmental samples³⁵⁻³⁸ and at high temperatures in highly corrosive solutions.¹⁸ With a view to the important role of pH in many physiological processes, we report here on a much improved fluorous-membrane ISE for measurements of pH.

Because pH is defined as the negative logarithm of the activity of H^+ and not as the logarithm of the H^+ concentration, ISEs have the intrinsic advantage that they measure the

activity of H^+ directly, which is difficult to do with other analytical techniques. However, the conventional glass electrodes have some disadvantages. Glass is a fragile material with high resistivity, which requires extra care when using glass electrodes and also limits uses of pH glass electrodes as part of miniaturized and implantable devices.³⁹ The use of pH glass electrodes in biological samples is hindered by protein adsorption onto the pH sensitive glass bulb, requiring frequent cleaning and maintenance,⁴⁰ and glass electrodes are not compatible with acidic samples that contain fluoride. To this end, H^+ -selective ISEs with polymeric sensing membranes have been developed. A wide range of electrically neutral ionophores with functional groups that can be protonated were successfully tested as H^+ -selective ionophores. Among them, the most successful ones are amine⁴¹⁻⁴² and pyridine⁴³⁻⁴⁴ derivatives.

Assuming the formation of 1:1 complexes between the ionophore and H^+ , two criteria were predicted to maximize the measuring range of such H^+ -selective ISEs:²² (1) The incorporation of ionophores and ionic sites at a 2:1 ratio, and (2) the use of hydrophobic matrixes with negligible cation binding properties. The latter criterion is met in an ideal manner by the fluorous matrixes of two fluorous-phase pH ISEs with the fluorophilic pH ionophores **1** and **3** (see Fig. 1), as reported previously.²⁸ While these two ISEs each covered a wide pH range, the one based on the more weakly binding H^+ ionophore (**1**) was limited to the acidic pH range, and the one based on the more strongly binding H^+ ionophore (**3**) was prone to Donnan failure. Herein, we report on an improved fluorous-phase pH ISE that offers a wide working range centered around pH 7. It is based on the new fluorophilic ionophore **2**, which has $-(\text{CH}_2)_4-$ spacers of optimized length between the proton-binding amino center of the ionophore and the perfluorooctyl groups that make this compound fluorophilic. We report here for the first time the synthesis of ionophore **2** by a step-wise alkylation method starting with ammonia and fluorinated

alkyl iodide. In comparison, the reported synthesis of ionophore **3** is more time-consuming due to the lack of commercially available starting materials.

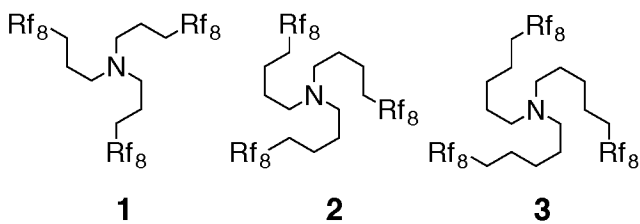


Figure 1. Structure formulas of the fluorophilic H⁺ ionophores **1** to **3**. Rf₈ = -(CF₂)₇CF₃.

We also describe in detail the redesign of an electrode body that provides significant improvements in reliability and is suitable not only for fluorous membranes but also any other stiff or fragile membrane material.

Experimental Section

Materials. All commercial reagents were of the highest purity available and used without purification. Perfluoroperhydrophenanthrene (**5**) and 1-iodo-4-(perfluoroctyl)butane (CF₃(CF₂)₇(CH₂)I) were purchased from SynQuest Lab (Alachua, FL) and Sigma Aldrich (St. Louis, MO), respectively. Sodium tetrakis[3,5-bis(perfluorohexyl)phenyl]borate (**4**) was synthesized according to a previously published procedure.²¹ EMD Millipore Fluoropore Polytetrafluoroethylene (PTFE) membrane filters (pore size 0.45 μ m, filter diameter 47 mm, thickness 50 μ m, 85% porosity) were purchased from Fisher Scientific (Hanover Park, IL). Viton fluoroelastomer O-rings were obtained from McMaster-Carr (Chicago, IL). Autonorm freeze-dried animal serum was purchased in powder form from Sero (Billingstad, Norway). High molecular weight poly(vinyl chloride), 2-nitrophenyl octyl ether (*o*-NPOE), tridodecylamine, and potassium tetrakis(4-chlorophenyl)borate were purchased from Sigma Aldrich (St. Louis, MO).

All aqueous solutions were prepared with deionized and charcoal-treated water ($0.182\text{ M}\Omega\text{ cm}$ specific resistance) from a Milli-Q Plus reagent-grade water system (Millipore, Bedford, MA).

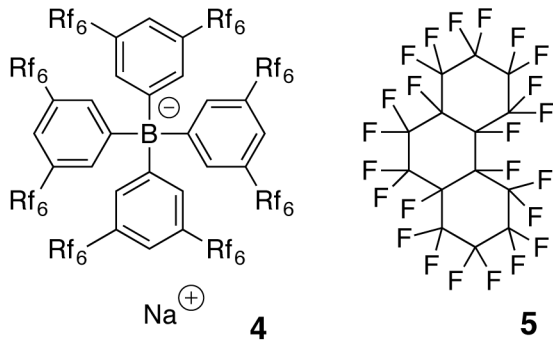


Figure 2. Structure formulas of the fluorophilic ionic site (**4**) and the fluorous matrix (**5**) of the fluorous-phase sensing membranes.

Synthesis of Ionophore $\text{N}[(\text{CH}_2)_4\text{R}_\text{f}]_3$ (2). The synthesis of ionophore **2** was performed using a modified literature procedure by stepwise alkylation of ammonia to a primary, secondary, and finally tertiary amine. This synthesis method was reported previously⁴⁵ for the preparation of other $\text{N}[(\text{CH}_2)_n\text{R}_\text{f}]_3$ compounds but has been used here for the first time for the synthesis of **2**. In view of applications in catalysis, **2** was prepared previously by oxidation of $\text{R}_\text{f}(\text{CH}_2)_4\text{OH}$ to the aldehyde, reductive amination with benzylamine, and deprotection to give a secondary amine, and finally a second reductive amination step to yield **2**.⁴⁶ Based on our own experience with both synthesis methods, the stepwise alkylation of ammonia with $\text{CF}_3(\text{CF}_2)_7(\text{CH}_2)_4\text{I}$ appears preferable for the preparation of **2** because it poses fewer challenges with the purification of intermediates.

$\text{CF}_3(\text{CF}_2)_7(\text{CH}_2)_4\text{I}$ (2.5 g) was dissolved in 3 ml tetrahydrofuran (THF) in a thick-walled test tube, which was then sealed with a rubber septum and cooled to $-78\text{ }^\circ\text{C}$ in an isopropanol/dry ice bath. Another thick-walled test tube was loaded with 3 mL THF, sealed with a rubber septum, and cooled to $-78\text{ }^\circ\text{C}$ with an isopropanol/dry ice bath, followed by

condensation of approximately 2 mL liquid ammonia from an ammonia tank into the THF. Then, the cooled liquid ammonia/THF solution was added into the cooled $\text{CF}_3(\text{CF}_2)_7(\text{CH}_2)_4\text{I}$ /THF solution through a cannula. For safety, this tube was placed into a closed plastic bottle as a secondary container. The reaction was stirred with a magnetic stir bar and allowed to warm gradually to room temperature, where it was stirred for another 48 h. In the post-reaction work-up, the solvent was removed, and the crude reaction mixture was re-dissolved in diethyl ether and washed with 1 M Na_2CO_3 solution. After washing of the aqueous phase three times with diethyl ether, the combined organic phases were dried over MgSO_4 , and the solvent was removed. The solid obtained thereby (1.4 g) was dissolved together with 2.0 g of $\text{CF}_3(\text{CF}_2)_7(\text{CH}_2)_4\text{I}$ and 0.2 g of Na_2CO_3 in 3 mL THF and heated under reflux for 3 days. After cooling to room temperature, the same post-reaction workup was repeated, giving 2.7 g of a solid. From this, 2.0 g were taken and dissolved together with 0.41 g of $\text{CF}_3(\text{CF}_2)_7(\text{CH}_2)_4\text{I}$ in THF and heated under reflux for 3 days. After cooling and evaporation of the THF, diethyl ether was added to give a suspension, which was filtered. The insoluble filtrate was washed three times with diethyl ether, and the four organic phases were combined and washed with 1 M Na_2CO_3 solution. The resulting aqueous phase was washed three times with diethyl ether, followed by combining of all organic phases and washing with brine and drying over MgSO_4 . After removal of the drying agent by filtration, the solvent was evaporated, and the product thus obtained was purified by column chromatography on silica gel with dichloromethane as eluent. This yielded $\text{N}[\text{CH}_2\text{CH}_2\text{CH}_2\text{CH}_2\text{R}_{\text{f}8}]_3$ (**2**) as a slightly yellow solid (460 mg, 23%). ^1H NMR (CDCl_3 , δ): 2.39 (t, 6H, N- CH_2 , $^3J_{\text{HH}} = 5$ Hz), 2.04–2.12 (m, 6H, $\text{CH}_2\text{R}_{\text{f}8}$), 1.48–1.63 (m, 12H, $\text{CH}_2\text{CH}_2\text{CH}_2\text{R}_{\text{f}8}$). MS: $[\text{M}-\text{H}]^+ = 1440.1$. For ^1H NMR and MS spectra, see Figs. S1 and S2 of the Supporting Information.

Fluorous-Phase Electrode Preparation. Solutions containing **2** (2 mM) and **4** (0.5 mM) in the fluorous matrix **5** were used for the fabrication of membranes for ionophore-based electrodes. Solutions of **4** (0.35 mM) in **5** were used for ionophore-free ion exchanger electrodes. In both cases, the solutions were stirred overnight with a magnetic stir bar at room temperature to ensure complete dissolution. To prepare sensing membranes, circular inert porous supports with a 19.1 mm diameter were cut from Fluoropore filters using a hole punch. Aliquots of 35 μ L of the fluorous solutions with **4** (and optionally **2**) were added onto the inert porous circular supports. This turned the initially solid white Teflon filter pieces transparent, showing that the fluorous solution had diffused into the pores of the support. In typical measurements, one layer of the Fluoropore support was used for each electrode. For measurements of tetraphenylphosphonium ion (PPh_4^+), tetrabutylammonium ion (NBu_4^+), and tetrapropylammonium ion (NPr_4^+) selectivities, 3 or 4 layers were used instead. This prevents these cations from diffusing through the fluorous sensing phase to the interface of the sensing membrane and inner filling solution and affecting the phase boundary potential at that interface within the time of the selectivity measurements. Filter disks impregnated with fluorous solution were mounted between the inner tube and the outer tube of the electrode body. An aqueous solution containing 10 mM K_2HPO_4 , 10 mM KH_2PO_4 , and 10 mM KCl (pH = 7.4) was used as inner filling solution. Note that in typical real-life applications, the sensing membrane is rarely challenged with solutions that result in a potentiometric response dominated by ions other than H^+ . For such applications, one layer of Teflon filter is sufficient. However, membranes with 3 or 4 layers of Teflon filters could be used routinely without any problems.

Electrode Bodies. In conventional ISEs with an inner filling solution, the sensing membrane separates the inner filling solution from the sample. Unlike in the case of plasticized

PVC membranes mounted into the well-known Philips-type electrode bodies,⁴⁷ sensing membranes supported by a Fluoropore filter cannot be bent into a cone shape by the electrode body, but instead the membrane must remain flat. In our previous design of electrode bodies for fluorous membranes,⁴⁸ the Fluoropore filter was sandwiched in between a screw cap and the electrode body. Every so often, the rotating motion in the assembly of the electrode caused an uneven seating of the sensing membrane and, consequently, leaking of the inner filling solutions and sub-Nernstian EMF responses. To eliminate this problem, a new electrode body was designed with an inner and an outer tube as well as a separate screw cap (Figure 3; see Figs. S3–S8 of the Supporting Information for further details).

With this new design, the sensing membrane is mounted in between the inner and outer tubes of the electrode body. The inner tube has two lugs that fit into the locking slots of the outer tube, preventing the inner tube from rotating with respect to the outer tube. Therefore, when the cap is screwed onto the outer tube, it exerts pressure onto the inner tube and presses it tightly against the membrane without exertion of rotating forces on the two flat O-rings and the membrane, thus providing a smooth and even seal. Note that the beveled shape of the outer tube adjacent to the sensing membrane prevents air bubbles from getting trapped at the edge of the membrane.

Measurements with the new electrode bodies showed much improved reliability. This design is based on simple engineering principles, can be easily reproduced in any machine shop, and may be readily adopted by other researchers. It is advantageous over gluing of PVC membranes onto Tygon or PVC tubing because insufficient or uneven application of THF (or a solution of PVC in THF) can lead to formation of leaks. Our design is also advantageous over the use of Philips electrode bodies⁴⁷ because, upon electrode assembly, it allows the sensing

membrane to keep its initial flat shape. In contrast, Philips electrode bodies force the sensing membrane into a cone shape, which can result in the formation of tears or wrinkles. While specifically developed by us for use with fluorous and other polymeric sensing membranes, we recently also used electrode bodies of this new design to hold rigid nanoporous glass frits,⁴⁹ which would have not been possible with Philips-type electrode bodies. This demonstrates the applicability of this new type of electrode body for a wider range of stiff or fragile membrane materials.

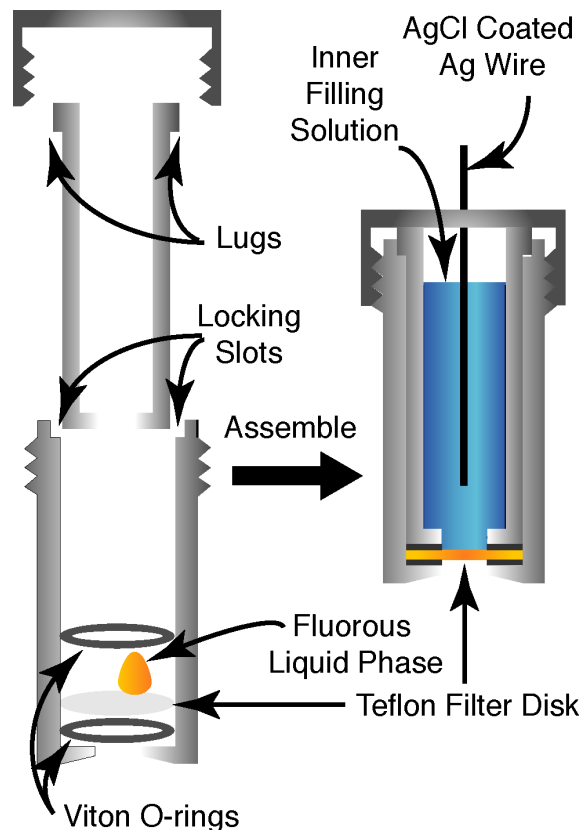


Figure 3. Design of an electrode body that avoids exertion of twisting forces on the sensing membrane during electrode assembly.

Preparation of ISEs with plasticized PVC membranes. Solutions to prepare PVC-phase pH membranes were prepared by slowly adding 66 mg PVC into a stirred solution of 132 mg *o*-NPOE in 1.0 mL THF, followed by addition of 13 mmol/kg potassium tetrakis(4-chlorophenyl)borate, and either 52 or 26 mmol/kg tridodecylamine to give an ionophore-to-ionic site ratio of 4:1 or 2:1, respectively (mmol/kg values refer to final concentration in the ISE membrane). Aliquots of these solutions were cast into a glass petri dish of 25 mm diameter, and the solvent was allowed to evaporate over 24 h, giving master membranes of 200 μ m thickness. Smaller circular disks of 7 mm were cut from master membranes and glued onto a Tygon tube using THF.

Potentiometric Measurements. Measurements were performed in stirred solutions with a 16-channel potentiometer (Lawson Labs, Malvern, PA) and a double junction free-flowing free-diffusion reference electrode (DX200, Mettler Toledo, Switzerland; Ag/AgCl as internal reference, AgCl-saturated 3 M KCl as inner solution, and 1M LiOAc as bridge electrolyte). The pH of sample solutions was changed stepwise by adding small aliquots of concentrated KOH or HCl solutions. A half-cell pH glass electrode (InLab 201, Mettler Toledo, Columbus, OH; calibrated with standard NIST pH buffers of pH 4.0, 7.0, 10.0, and 12.0) was used to monitor separately the pH. Selectivity coefficients were determined for K^+ , Na^+ , and Ca^{2+} with the fixed interference method (FIM) and for NPr_4^+ with respect to NBu_4^+ and for NBu_4^+ with respect to PPh_4^+ with the separate solution method (SSM; see the Supporting Information for further details).^{27, 29} Nernstian slopes were confirmed in all cases. All response times in the Nernstian response region were fast (< 5 s). Activities were calculated with a two-parameter Debye–Hückel approximation.⁵⁰

Conductivity Measurements. The conductivities of membranes at five different concentrations of ionophore and ionic site were measured using the known shunt method.^{21, 48, 51-52} An ionophore to ionic site ratio of 4:1 was used for all five concentration levels. The inner filling and measuring solutions contained 10 mM K₂HPO₄, 10 mM KH₂PO₄, and 10 KCl mM (pH = 7.4). Conductivity values were calculated based on an estimated cell constant of 0.00924 cm⁻¹.

Results and Discussion

Response Range of ISEs with the New Ionophore

Calibration curves of fluorous-phase ISEs with the new ionophore were obtained with a constant background consisting of 970 mM KCl and 20 mM phosphate buffer (initially at pH 7.4) by addition of KOH or HCl aliquots. A typical calibration curve in the range between pH 0 and 14 is shown in Figure 4. As can be seen, even in an electrolyte solution with such a high concentration of an interfering cation with a relatively low hydration energy as K⁺, the new ionophore **2** has a wide working range from pH = 2.2 to pH = 11.2, centered near pH 7 and with a slope of 54.7 ± 0.7 mV/decade ($n = 3$). This fits the need for a single sensor that is capable of measuring a range of biological samples.

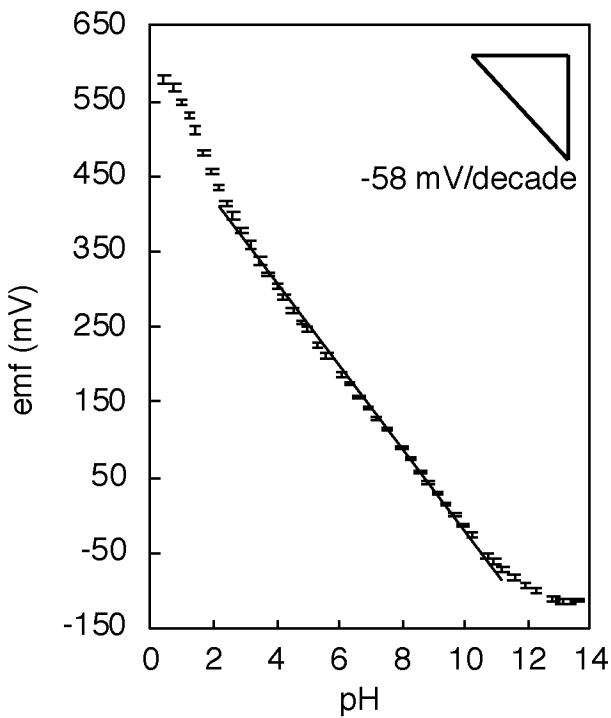


Figure 4. Working range of pH ISEs based on ionophore **2**: EMF measurements were started at pH 7.4 (970 mM KCl, 10 mM K₂HPO₄, and 10 mM KH₂PO₄ solution). The pH was increased by adding small aliquots of 10 M KOH solution. Subsequently, starting again at pH 7.4, the pH was decreased by adding aliquots of 1 M HCl solution. Shown are only error bars (n=3); symbols for emf averages are not shown to avoid overlap of the very narrow error ranges with such symbols. The 1.0 M total K⁺ ion background was selected to match the testing conditions of ionophore **3** as reported in ref. 28 and, thereby, make results directly comparable. The accuracy of the pH was estimated by division of the root mean square deviation (RMSD) from a linear regression by the response slope, giving 0.036 for the range from pH 4.2 to pH 11.0 and 0.0056 for the range pH 6.1 to pH 8.0.

Fluorous-phase ISEs with either one of the structurally closely related fluorophilic trialkylamines **1** or **3** as ionophore were reported previously.²⁸ The three C₈F₁₇ chains that all these ionophores share, also referred to as “fluorophilic ponytails,” are necessary to make these ionophores sufficiently soluble in fluorous phases. However, ionophores **1** and **3** differ in the number of -CH₂- groups that separate the nitrogen center from the highly electron withdrawing fluorophilic ponytails. As shown previously in a potentiometric study that included among other compounds **1** and **3** but not **2**,²⁸ the longer the -(CH₂)_n- spacers are, the better they shield the nitrogen atom from the electron withdrawing effect of the perfluoroalkyl groups, therefore, and the more basic the ionophores are. Variation of the -(CH₂)_n- spacer is an efficient way to adjust the pK_a value and, thereby, the selectivity of the ionophore. Gas phase ionization data illustrate this effect. While corresponding data for N[(CH₂)_nR_{f8}]₃ compounds are not available, the experimental ionization potentials for P[(CH₂)_nR_{f8}]₃ decrease stepwise by 0.37, 0.26, and 0.1 eV going from n = 2 to 3, 4, and 5, respectively.⁵³ Also, calculated gas phase proton affinities for NH₂[(CH₂)_nCF₂CF₃] were reported to increase stepwise from n = 2 to 3, 4, and 5 by 4.4, 2.0, and 1.7 kcal/mol, respectively.⁴⁵ These data suggest that the pK_a of **2** similarly lies between the pK_a values of **1** and **3** but is closer to the pK_a of **3** than to the pK_a of **1**.

This is important because the upper and lower detection limits of an ionophore-based pH ISE both depend on the basicity of the ionophore (i.e., the pK_a of ionophore-H⁺ complex). The upper detection limit also depends on the activities and lipophilicities of the counter ions in the sample, and the lower detection limit is also affected by the activities and lipophilicities of interfering ions. However, in the determination of the overall width of the working range, as defined by the difference between the upper and lower detection limits and referred to here as ΔpH, the K_a terms have been reported to cancel one another.²² Bakker et al., who proposed this

model, experimentally confirmed its validity for ISEs with plasticized PVC membranes.²² Importantly, according to this model, the working range is not expected to depend on the pK_a of the ionophore. When switching between ionophores differing in pK_a , both the upper and lower detection limits are expected to shift in the same pH direction, and the overall width of the working range remains unchanged.

In contradiction to these expectations, the working ranges of ISEs based on the fluorophilic ionophores **1** and **3** were reported to be 5 pH units (pH 1.5 to 6.5) and 8 pH units (pH 5.0 to 13.0), respectively.²⁸ In both cases, the ionophore to ionic site ratio was 2:1, and the working ranges were determined in the same background, i.e., 1 M KCl with a low concentration of tris(hydroxymethyl)aminomethane as pH buffer to facilitate measurements in the neutral pH range. Since the lower detection limit (at high pH) is determined for both ionophores by the H^+ vs K^+ selectivity, as apparent by the emf leveling off with the 1 M KCl background, the difference in the working ranges of these two ionophores comes from the upper detection limit (that is, low pH). At the upper detection limit, in contrast to a leveling off of the emf response as it is typically expected for the onset of Donnan failure,²⁵⁻²⁸ super-Nernstian responses were observed. The reason for the super-Nernstian response is not known but may be related to formation of H^+ –ionophore complexes with stoichiometries other than 1:1 as Donnan failure sets in. Note that a similar small super-Nernstian response was also observed for ionophore **2**, but only below pH 2 (see Figure 4).

For this reason, an ionophore to ionic site ratio of 4:1 was used in this work, ensuring that the formation of complexes of higher stoichiometry would not result in a very low concentration of free ionophore in the bulk of the sensing membrane. In addition, in an attempt to minimize

interference from buffer ion interference at low pH, the highly hydrophilic phosphate was used for the pH buffer rather than the tris(hydroxymethyl)aminomethane used previously.

As Figure 4 shows, the linear response range of the ISE with this new ionophore (pH 2.2 to 11.2) meets the need for a working range centered around pH 7, as desired for most biological samples. It resolves the shortcomings in both of the two previously reported fluorophilic ionophores **1** and **3**. ISEs based on the ionophore **1** evidently fail in the neutral pH region, where most of biological samples fall into, such as blood (pH 7.3–7.4), urine (pH 5.0–8.0) and saliva (pH = 6.4–7.0).⁵⁴ ISEs based on ionophore **3** cover a wide pH range from neutral to basic pH but depending on the type of counter ions in the sample are more likely to fail in even moderately acidic solutions. These drawbacks are overcome by the new fluorophilic H⁺ ionophore **2**.

Potentiometric Selectivity

The selectivities of many ionophore-based H⁺ selective electrodes have been reported in the literature, most commonly with respect to K⁺, Na⁺, and Ca²⁺ because of the relevance of these ions for clinical tests. Because sample solutions that contain no H⁺ cannot be prepared, selectivity coefficients for H⁺ selective ISEs are usually determined with the fixed interfering method.^{27, 29} Figure 5 shows for ISEs with **2** as ionophore the pH calibration curves measured in a constant background of K⁺, Na⁺, or Ca²⁺. Corresponding selectivity coefficients are listed in Table 1, along with selectivities for ISEs based on ionophores **1** and **3**.²⁸

As the table and figure show, the new fluorous-phase pH electrode has a high selectivity with respect to all three interfering ions. Even in presence of 1 M K⁺ and Na⁺, the electrode starts to respond to interfering ions only at pH ≈12 ($\log K_{\text{H,K}}^{\text{pot}} = -11.6$, $\log K_{\text{H,Na}}^{\text{pot}} = -12.4$). Because in the sequence of ionophores **1**, **2**, and **3** the length of the spacers separating the perfluoroalkyl

groups from the nitrogen center increases from $-(\text{CH}_2)_3-$ to $-(\text{CH}_2)_4-$ and $-(\text{CH}_2)_5-$, the stability of the H^+ complexes and the selectivities of the corresponding ISEs are expected to increase steadily from **1** to **3**. This expectation is confirmed by the selectivities for H^+ with respect to both Na^+ and K^+ (see Table 1). Note that Ca^{2+} precipitation prevented the observation of Ca^{2+} interference for ISEs based on ionophore **2**. The electrodes responded perfectly linear all the way to pH 12.2, which permits only specification of an upper limit of the selectivity coefficient (i.e., $\log K_{\text{H,Ca}}^{\text{pot}} < -10.2$).

Table 1. Selectivities and Working Ranges of ISEs based on Ionophores **1**, **2**, and **3**.

	Ionophore		
	1 ^a	2 ^b	3 ^a
$\log K_{\text{H,K}}^{\text{pot}}$	-7.9	-11.6	< -12.8
$\log K_{\text{H,Na}}^{\text{pot}}$	-9.3	-12.4	< -13.8
$\log K_{\text{H,Ca}}^{\text{pot}}$	-6.7	< -10.2	< -10.8
Working Range	1.5 – 6.5	2.2 – 11.2	5.0 – 13.0
$\text{p}K_a$	9.8	15.8	15.4

^a See reference 28. ^b This work. Experimentally observed standard deviations: 0.1 in $\log K_{\text{H,K}}^{\text{pot}}$ and $\log K_{\text{H,Na}}^{\text{pot}}$; 0.01 in $\log K_{\text{H,Ca}}^{\text{pot}}$ ($n=3$).

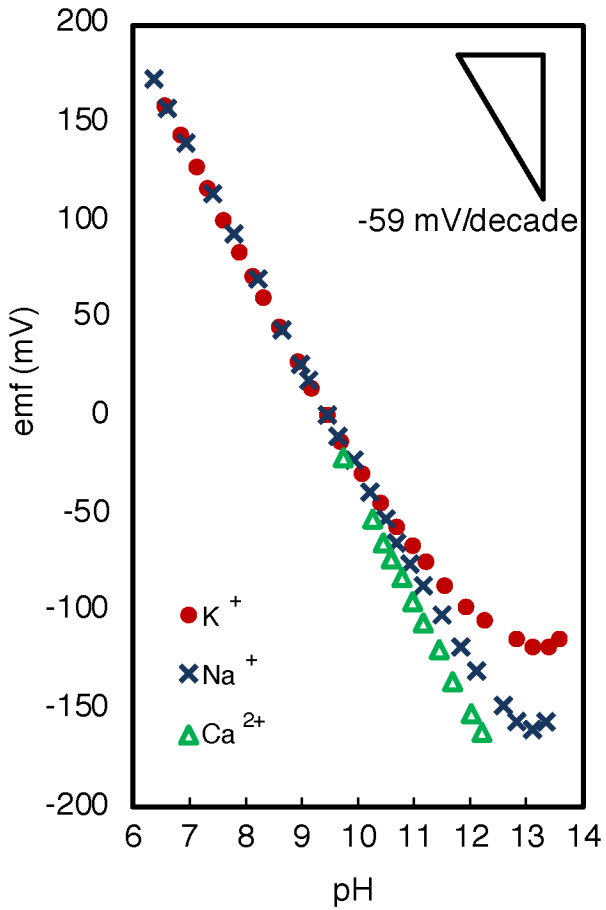


Figure 5. EMF response to pH with a constant metal ion concentration, demonstrating the high selectivity of ISEs based on ionophore **2** for H^+ with respect to K^+ , Na^+ , and Ca^{2+} . Selectivities with respect to K^+ and Na^+ were measured in a constant 1 M K^+ and 1 M Na^+ background, respectively (K^+ or Na^+ salts of 10 mM HPO_4^{2-} , 10 mM H_2PO_4^- , and 970 mM Cl^-). The pH was gradually increased by addition of 10 M KOH or NaOH aliquots. The response to Ca^{2+} was measured with a constant 10 mM Ca^{2+} background; measurements were started with 10 mM $\text{Ca}(\text{OH})_2$, and the pH was gradually decreased by adding aliquots of a solution that contained 3 M HCl and 10 mM CaCl_2 .

Basicity of Fluorophilic H^+ Ionophores

As the basicity of an ionophore dictates to a large extent the selectivity and working range of ionophore-based pH ISEs, it was of interest to determine the effect of the $-(\text{CH}_2)_4-$

spacers on the pK_a value of the new fluorophilic pH ionophore **2**. Two common methods to determine the stability of the complexes between ionophores and ions (and, in the case of a H^+ ionophore, the pK_a of the ionophore– H^+ complex) are the so-called “sandwich membrane method”^{55–57} and the spectrophotometric method.⁵⁸ Neither of them is suitable for the fluorous ISE membranes of this work. The former method is not applicable to ISEs with a non-polymeric sensing phase because it requires membranes in which ions diffuse only slowly, and the latter method requires a fluorophilic chromoionophore, which is not currently available. Therefore, the pK_a value of the fluorophilic ionophore **2** was determined here by measurements of the selectivity with respect to an ion that was assumed not to bind to the ionophore.^{59–61} Specifically, using this approach, the selectivity coefficient of an ionophore-doped membrane for a non-coordinating ion (J^+) with respect to the primary ion (H^+), $\log K_{H,J}^{\text{pot}}(L)$, is compared to the corresponding selectivity coefficient of an ionophore-free ion-exchanger membrane, $\log K_{H,J}^{\text{pot}}(\text{IE})$. (For a definition of ionophore-free ion-exchanger membranes, see ref. 8, p 1595.) By insertion of these selectivity coefficients, the total ionophore concentration, L_T , and the total ionic site concentration, R_T , into eq 1, the apparent complex conformation constant between the ionophore and the primary ion, β_{HL} , can be calculated.

$$\beta_{HL} = \frac{K_{H,J}^{\text{pot}}(L)}{K_{H,J}^{\text{pot}}(\text{IE})} \frac{\log K_{H,J}^{\text{pot}}(L) - \log K_{H,J}^{\text{pot}}(\text{IE})}{[L_T - R_T] \log K_{H,J}^{\text{pot}}(L) + R_T \log K_{H,J}^{\text{pot}}(\text{IE})} \quad (1)$$

In view of the exceptionally low polarity and polarizability of fluorous phases, the selectivity coefficients needed to be corrected for ion pair formation, though. The difference between the free H^+ concentration in the ionophore-doped and ionophore-free membranes is not only caused by the ionophore. There is also a different extent of ion pair formation in the two types of membranes. Specifically, ion pair bonding between the ionic sites and the rather large

ionophore–H⁺ complex is expected to be weaker than ion pair bonding between the ionic sites and H⁺, even if the latter is partially hydrated. Ion pair formation constants can be obtained from the conductivity of membranes that contain the ionic site and either H⁺ or ionophore–H⁺ complexes at different concentrations. Fitting the experimentally determined conductivities with the Fuoss–Kraus equation (eq 2) affords the ion pair formation constant.⁶²

$$\Lambda = \frac{\Lambda_s^\infty}{c^{1/2} K_{ip}^{1/2}} + \frac{2\Lambda_s^\infty c^{1/2} K_t}{3K_{ip}^{1/2}} \quad (2)$$

Λ and c are the conductivity and salt concentration, respectively, Λ_s^∞ is the limiting molar conductivity of the undissolved salt, and K_{ip} and K_t are the formation constants of the ion pairs and triple ions, respectively. For example, the logarithm of the ion pair formation constant between the ionic site and the complex of ionophore **2** and H⁺, $\log K_{ip,H^+}$, was thus determined to be 12.8 ± 0.1 . Subsequently, selectivity coefficients corrected for ion pairing using eq 3 were inserted into eq 1 to afford pK_a values of ionophore–H⁺ complexes corrected for ion pairing

$$\log K_{H,J}^{\text{pot,corr}}(L) = \log K_{H,J}^{\text{pot}}(L) - (\log K_{ip,J} - \log K_{ip,H^+}) \quad (3)$$

Stabilities of ion pairs between the ionic site and non-coordinating ions J , $K_{ip,J}$, and selectivity coefficients of ionophore-free ion-exchanger membranes were adopted from ref. 21. K⁺ was assumed to be a non-coordinating ion. Selectivity coefficients for K⁺ with respect to H⁺ were directly measured with the fixed interference method.

Correction for ion pair formation gave the pK_a value for ionophore **2** as 15.8 ± 1.2 , which is substantially larger than the previously reported pK_a of 9.8 for ionophore **1** and, therefore, is consistent with the ability of the longer -(CH₂)₄- spacer of **2** to shield the amino center from electron-withdrawing perfluorooctyl groups. However, we were surprised that the pK_a value determined here for ionophore **2** is slightly higher than the previously reported value for ionophore **3**. We suspect that this discrepancy comes from an artifact in the conductivity

measurements reported in ref. 28, which resulted in an underestimation of the previously reported pK_a of **3**. The conductivity measurements used to determine the pK_a of ionophores **3** were made at pH = 3 with an ionophore to ionic site ratio of 2:1. This is not an ideal pH for ionophore **3**, since ISEs based on this ionophore exhibit a super-Nernstian response at this pH. This adds uncertainty to the ion pair formation constant and, consequently, the determination of the pK_a value. The formation of H^+ -ionophore complexes of 2:1 stoichiometry and ion aggregates larger than triple ions⁶³⁻⁶⁴ may also affect the accuracy of pK_a values of ionophores in ISE membranes.

Improved Resistance of Fluorous-Phase Ion-Selective Electrodes to Biofouling

The uniqueness of fluorous-phase ISEs comes from the extremely non-polar nature of their membrane matrixes.³⁰⁻³¹ Fluorous matrixes are both hydrophobic and lipophobic, which minimizes the solvation of interfering species, and in particular of lipophilic species from biological samples. To demonstrate the potential of fluorous membranes to resist biofouling, three types of electrodes were calibrated in aqueous buffer solutions from pH 7 to pH 14, namely, fluorous-phase pH electrodes with an ionophore-to-ionic-site ratio of 4 to 1 as well as pH electrodes with a plasticized PVC membranes doped with ionophore-to-ionic-site ratios of 4 to 1 and 2 to 1. Then all three types of electrodes were stored in 10% serum solutions for five days (120 h) before they were calibrated again in the same fashion in aqueous solutions. All three types of electrodes were calibrated, stored, and calibrated again at the same time and in the same container to ensure the rigor of this comparison. The calibration plots of the fluorous-phase pH electrodes with the 4 to 1 ionophore-to-ionic-site ratio and the PVC-phase pH electrodes with the 2 to 1 ionophore-to-ionic-site ratio, each before and after serum exposure, are shown in Figure 6.

Fluorous-phase pH electrodes maintained their good H^+ selectivity against K^+ after exposure to 10% serum (selectivity coefficients $\log K_{\text{H},\text{K}}^{\text{pot}}$ as determined before and after serum exposure were -11.3 ± 0.4 and -11.4 ± 1.0 , respectively; $n = 3$). In contrast, the selectivity of the PVC-phase pH electrodes with the 4 to 1 ionophore-to-ionic-site ratio worsened slightly from -11.6 ± 0.1 to -11.3 ± 0.1 ($n = 3$), and the selectivity of PVC-phase pH electrodes with the 2 to 1 ionophore-to-ionic-site ratio suffered an even larger loss of selectivity by 0.56 logarithmic units (from -11.1 ± 0.1 to -10.6 ± 0.1 ; $n = 4$). This finding is consistent with an improved resistance to biofouling of fluorous-phase pH ISEs.

On a side note, we would also like to point out the slightly higher selectivity of the PVC-phase pH electrodes with the 4 to 1 ionophore-to-ionic-site ratio as compared to electrodes with the same membrane matrix but a 2:1 ionophore-to-ionic-site ratio. The ISE literature has typically assumed 1:1 complex formation between H^+ and trialkylamine ionophores. We first started to suspect that trialkylamine ionophore may also form 2:1 complexes when we worked with fluorous ionophore-doped membranes and noted the superior performance of membranes with the 4 to 1 ionophore-to-ionic-site ratio.¹⁸ Note that when (i) an ISE membrane contains ionophore and ionic sites in a 2:1 ratio and (ii) the ionophore forms a very stable 2:1 complex with the H^+ , the membrane, the concentration of free ionophore in this membrane is very low, resulting in reduced potentiometric selectivity. The data presented suggest that this effect is indeed occurring in PVC-phase ISEs, providing for a not insignificant improvement in selectivity for the membranes with the 4:1 ionophore-to-ionic-site ratio. It is conceivable that this same effect may also apply to H^+ ionophores other than trialkylamines, many of which may also form not only 1:1 but also 2:1 complexes with H^+ .⁶⁵

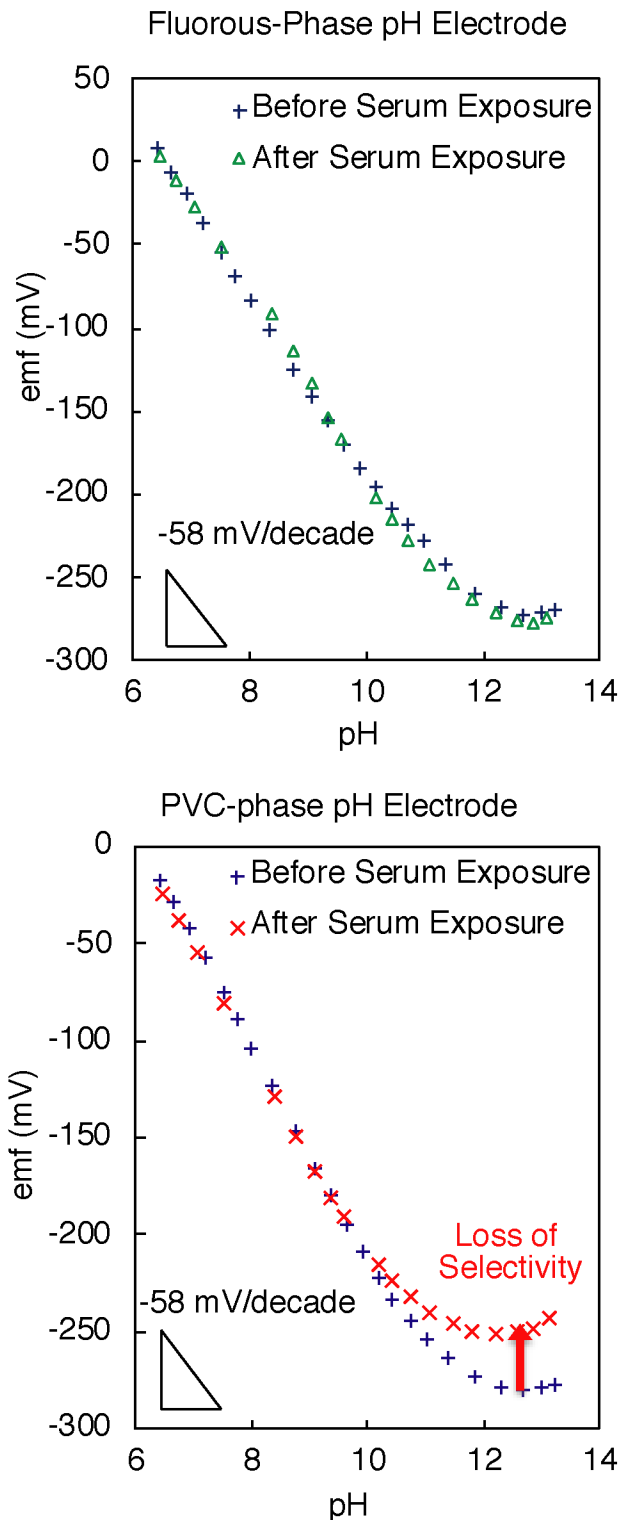


Figure 6. Calibration of fluorous-phase pH electrodes with the 4 to 1 ionophore-to-ionic-site ratio and PVC-phase pH electrodes with the 2 to 1 ionophore-to-ionic site ratio, each before and

after serum exposure. EMF measurements were started at pH 7.4 (970 mM KCl, 10 mM K₂HPO₄, and 10 mM KH₂PO₄ solution). The pH was increased by adding small aliquots of 10 M KOH solution. The pH accuracies (RMSD/slope) as calculated from the root mean square deviation (RMSD) of the linear regression before and after serum exposure are 0.03 and 0.03, respectively, for the fluorous-phase ISEs (top panel) and 0.021 and 0.026, respectively, for the PVC membrane ISEs with the 2 to 1 ionophore-to-ionic-site ratio (bottom panel).

Conclusions

In previous work, the unique low polarity of fluorous sensing membranes allowed the preparation of H⁺ selective ISEs based on ionophore **3** with an extremely high selectivity. However, their detection limit at low pH was compromised by too high an affinity of the ionophore for H⁺. In contrast, ISEs based on ionophore **1** exhibited lower selectivities due to a too low H⁺ affinity. In this work, we optimized the affinity of the ionophore for H⁺ and demonstrated that ISEs with the new fluorophilic ionophore **2** have a wide working range centered around the physiologically important pH 7. Measurements in biological samples demonstrated the improved ability of these fluorous-phase ISEs to maintain a high selectivity after exposure to 10% serum for 5 days. We also found evidence that a 2:1 ionophore-to-ionic-site ratio is too low for the optimum use of trialkylamine ionophores for H⁺, but further study will be needed to establish how matrix-dependent this effect is, and whether this is also true for other H⁺ ionophores.

Author Information

Corresponding Author

*E-mail: Buhlmann@umn.edu. Tel: +1 (612) 624-1431.

ORCID

Xin V. Chen: 0000-0003-4477-043X

Philippe Bühlmann: 0000-0001-9302-4674

Acknowledgements

This work was supported by the National Science Foundation (CHE-1748148). We thank Peter Ness from the College of Science and Engineering Machine Shop, University of Minnesota, for help with the design and fabrication of the electrode bodies and Dr. Aniko Nemes, Department of Chemistry, Eötvös Loránd University, for helpful discussions on the topic of organic synthesis. M. P. S. M. was supported by a University of Minnesota Doctoral Dissertation Fellowship.

Supporting Information

¹H NMR and mass spectra of ionophore **2**. Details of electrode body design, including dimensions. Details of the selectivity determination. Working range of three individual pH ISEs based on ionophore **2**. This material is available free of charge via the Internet at <http://pubs.acs.org>.

References

1. Bobacka, J.; Ivaska, A.; Lewenstam, A., Potentiometric Ion Sensors. *Chem. Rev.* **2008**, *108*, 329-351.
2. Michalska, A., All-Solid-State Ion Selective and All-Solid-State Reference Electrodes. *Electroanalysis* **2012**, *24*, 1253-1265.
3. Crespo, G. A.; Bakker, E., Dynamic Electrochemistry with Ionophore Based Ion-Selective Membranes. *RSC Adv.* **2013**, *3*, 25461-25474.
4. Yin, T. J.; Qin, W., Applications of Nanomaterials in Potentiometric Sensors. *TrAC, Trends Anal. Chem.* **2013**, *51*, 79-86.

5. Bakker, E., Potentiometric Sensors. In *Environmental Analysis by Electrochemical Sensors and Biosensors: Fundamentals*, Moretto, L. M.; Kalcher, K., Eds. Springer: New York, NY, 2014; pp 193-238.
6. Bühlmann, P.; Chen, L. D., Ion-Selective Electrodes With Ionophore-Doped Sensing Membranes. In *Supramolecular Chemistry: From Molecules to Nanomaterials*, Jonathan, W.; Steed, P. A. G., Eds. John Wiley & Sons: New York, NY, 2012; Vol. 5, pp 2539-2580.
7. Bakker, E.; Bühlmann, P.; Pretsch, E., Carrier-Based Ion-Selective Electrodes and Bulk Optodes. 1. General Characteristics. *Chem. Rev.* **1997**, *97*, 3083-3132.
8. Bühlmann, P.; Pretsch, E.; Bakker, E., Carrier-Based Ion-Selective Electrodes and Bulk Optodes. 2. Ionophores for Potentiometric and Optical Sensors. *Chem. Rev.* **1998**, *98*, 1593-1688.
9. Sokalski, T.; Ceresa, A.; Zwickl, T.; Pretsch, E., Large Improvement of the Lower Detection Limit of Ion-Selective Polymer Membrane Electrodes. *J. Am. Chem. Soc.* **1997**, *119*, 11347-11348.
10. Ceresa, A.; Radu, A.; Peper, S.; Bakker, E.; Pretsch, E., Rational design of potentiometric trace level ion sensors. A Ag^+ -selective electrode with a 100 ppt detection limit. *Anal. Chem.* **2002**, *74*, 4027-4036.
11. Qin, W.; Zwickl, T.; Pretsch, E., Improved Detection Limits and Unbiased Selectivity Coefficients Obtained by Using Ion-Exchange Resins in the Inner Reference Solution of Ion Selective Polymeric Membrane Electrodes. *Anal. Chem.* **2000**, *72*, 3236-3240.
12. Bakker, E.; Pretsch, E., Potentiometry at Trace Levels. *TrAC, Trends Anal. Chem.* **2001**, *20*, 11-19.
13. Malon, A.; Vigassy, T.; Bakker, E.; Pretsch, E., Potentiometry at Trace Levels in Confined Samples: Ion-Selective Electrodes with Subfemtomole Detection Limits. *J. Am. Chem. Soc.* **2006**, *128*, 8154-8155.
14. Lai, C. Z.; Fierke, M. A.; da Costa, R. C.; Gladysz, J. A.; Stein, A.; Bühlmann, P., Highly Selective Detection of Silver in the Low PPT Range with Ion-Selective Electrodes Based on Ionophore-Doped Fluorous Membranes. *Anal. Chem.* **2010**, *82*, 7634-7640.
15. Zou, X. U.; Cheong, J. H.; Taitt, B. J.; Bühlmann, P., Solid Contact Ion-Selective Electrodes with a Well-Controlled Co(II)/Co(III) Redox Buffer Layer. *Anal. Chem.* **2013**, *85*, 9350-9355.
16. Bakker, E., Can Calibration-Free Sensors Be Realized? *ACS Sens.* **2016**, *1*, 838-841.
17. Rumpf, G.; Spicher-Keller, U.; Bühlmann, P., Calibration-Free Measurement of Sodium and Potassium in Undiluted Human Serum with an Electrically Symmetrical Measuring System. *Anal. Sci.* **1992**, *8*, 553-559.
18. Lugert-Thom, E. C.; Gladysz, J. A.; Rabai, J.; Bühlmann, P., Cleaning of pH Selective Electrodes with Ionophore-doped Fluorous Membranes in NaOH Solution at 90 °C. *Electroanalysis* **2018**, *30*, 611-618.
19. Bariya, M.; Nyein, H. Y. Y.; Javey, A., Wearable Sweat Sensors. *Nat. Electron.* **2018**, *1*, 160-171.
20. Bandodkar, A. J.; Molinnus, D.; Mirza, O.; Guinovart, T.; Windmiller, J. R.; Valdes-Ramirez, G.; Andrade, F. J.; Schonning, M. J.; Wang, J., Epidermal Tattoo Potentiometric Sodium Sensors With Wireless Signal Transduction for Continuous Non-Invasive Sweat Monitoring. *Biosens. Bioelectron.* **2014**, *54*, 603-609.
21. Boswell, P. G.; Bühlmann, P., Fluorous Bulk Membranes for Potentiometric Sensors with Wide Selectivity Ranges: Observation of Exceptionally Strong Ion Pair Formation. *J. Am. Chem. Soc.* **2005**, *127*, 8958-8959.

22. Bakker, E.; Xu, A. P.; Pretsch, E., Optimum Composition of Neutral Carrier Based pH Electrodes. *Anal. Chim. Acta* **1994**, *295*, 253-262.

23. Morf, W. E.; Kahr, G.; Simon, W., Reduction of Anion Interference in Neutral Carrier Liquid-Membrane Electrodes Responsive to Cations. *Anal. Lett.* **1974**, *7*, 9-22.

24. Buck, R. P.; Toth, K.; Graf, E.; Horvai, G.; Pungor, E., Donnan Exclusion Failure in Low Anion Site Density Membranes Containing Valinomycin. *J. Electroanal. Chem.* **1987**, *223*, 51-66.

25. Bühlmann, P.; Amemiya, S.; Yajima, S.; Umezawa, Y., Co-Ion Interference for Ion-Selective Electrodes Based on Charged and Neutral Ionophores: A Comparison. *Anal. Chem.* **1998**, *70*, 4291-4303.

26. Ogawara, S.; Carey, J. L.; Zou, X. U.; Bühlmann, P., Donnan Failure of Ion-Selective Electrodes with Hydrophilic High-Capacity Ion-Exchanger Membranes. *ACS Sens.* **2016**, *1*, 95-101.

27. Buck, R. P.; Lindner, E., Recommendations for Nomenclature of Ion-Selective Electrodes - (IUPAC Recommendations 1994). *Pure Appl. Chem.* **1994**, *66*, 2527-2536.

28. Boswell, P. G.; Szíjjártó, C.; Jurisch, M.; Gladysz, J. A.; Rábai, J.; Bühlmann, P., Fluorophilic Ionophores for Potentiometric pH Determinations with Fluorous Membranes of Exceptional Selectivity. *Anal. Chem.* **2008**, *80*, 2084-2090.

29. Bakker, E.; Pretsch, E.; Bühlmann, P., Selectivity of Potentiometric Ion Sensors. *Anal. Chem.* **2000**, *72*, 1127-1133.

30. Horváth, I. T.; Rábai, J., Facile Catalyst Separation Without Water: Fluorous Biphase Hydroformylation of Olefins. *Science* **1994**, *266*, 72-75.

31. Gladysz, J. A.; Curran, D. P.; Horváth, I. T., *Handbook of Fluorous Chemistry*. Wiley & Sons: New York, 2005.

32. Chen, L. D.; Mandal, D.; Pozzi, G.; Gladysz, J. A.; Bühlmann, P., Potentiometric Sensors Based on Fluorous Membranes Doped with Highly Selective Ionophores for Carbonate. *J. Am. Chem. Soc.* **2011**, *133*, 20869-20877.

33. Lai, C.-Z.; Koseoglu, S. S.; Lugert, E. C.; Boswell, P. G.; Rábai, J.; Lodge, T. P.; Bühlmann, P., Fluorous Polymeric Membranes for Ionophore-Based Ion-Selective Potentiometry: How Inert Is Teflon AF? *J. Am. Chem. Soc.* **2009**, *131*, 1598-1606.

34. Carey, J. L.; Hirao, A.; Sugiyama, K.; Bühlmann, P., Semifluorinated Polymers as Ion-Selective Electrode Membrane Matrixes. *Electroanalysis* **2017**, *29*, 739-747.

35. Gunsolus, I. L.; Mousavi, M. P. S.; Hussein, K.; Bühlmann, P.; Haynes, C. L., Effects of Humic and Fulvic Acids on Silver Nanoparticle Stability, Dissolution, and Toxicity. *Environ. Sci. Technol.* **2015**, *49*, 8078-86.

36. Mousavi, M. P. S.; Gunsolus, I. L.; Pérez De Jesús, C. E.; Lancaster, M.; Hussein, K.; Haynes, C. L.; Bühlmann, P., Dynamic Silver Speciation as Studied with Fluorous-Phase Ion-Selective Electrodes: Effect Of Natural Organic Matter on the Toxicity and Speciation of Silver. *Sci. Total Environ.* **2015**, *537*, 453-461.

37. Chen, L. D.; Lai, C. Z.; Granda, L. P.; Fierke, M. A.; Mandal, D.; Stein, A.; Gladysz, J. A.; Bühlmann, P., Fluorous Membrane Ion-Selective Electrodes for Perfluorinated Surfactants: Trace-Level Detection and in Situ Monitoring of Adsorption. *Anal. Chem.* **2013**, *85*, 7471-7477.

38. Maurer-Jones, M. A.; Mousavi, M. P. S.; Chen, L. D.; Bühlmann, P.; Haynes, C. L., Characterization of Silver Ion Dissolution from Silver Nanoparticles using Fluorous-Phase Ion-Selective Electrodes and Assessment of Resultant Toxicity to *Shewanella Oneidensis*. *Chem. Sci.* **2013**, *4*, 2564-2572.

39. Ammann, D., *Ion-Selective Microelectrodes: Principles, Design and Application*. Springer: New York, 1986; Vol. 50.

40. Simon, W.; Ammann, D.; Anker, P.; Oesch, U.; Band, D. M., Ion-Selective Electrodes and Their Clinical-Application in the Continuous Ion Monitoring. *Ann. N.Y. Acad. Sci.* **1984**, 428, 279-285.

41. Anker, P.; Ammann, D.; Simon, W., Blood-pH Measurement with a Solvent Polymeric Membrane-Electrode in Comparison with a Glass-Electrode. *Mikrochim. Acta* **1983**, 1, 237-242.

42. Espadas-Torre, C.; Bakker, E.; Barker, S.; Meyerhoff, M. E., Influence of Nonionic Surfactants on the Potentiometric Response of Hydrogen Ion-Selective Polymeric Membrane Electrodes. *Anal. Chem.* **1996**, 68, 1623-1631.

43. Chao, P.; Ammann, D.; Oesch, U.; Simon, W.; Lang, F., Extracellular and Intracellular Hydrogen Ion-Selective Microelectrode Based on Neutral Carriers with Extended pH Response Range in Acid-Media. *Pfluegers Arch.* **1988**, 411, 216-219.

44. Dinten, O.; Spichiger, U. E.; Chaniotakis, N.; Gehrig, P.; Rusterholz, B.; Morf, W. E.; Simon, W., Lifetime of Neutral-Carrier-Based Liquid Membranes in Aqueous Samples and Blood and The Lipophilicity of Membrane-Components. *Anal. Chem.* **1991**, 63, 596-603.

45. Szlavik, Z.; Tarkanyi, G.; Gomory, A.; Tarczay, G.; Rabai, J., Convenient Syntheses and Characterization of Fluorophilic Perfluoroctyl-Propyl Amines and Ab Initio Calculations of Proton Affinities of Related Model Compounds. *J. Fluorine Chem.* **2001**, 108, 7-14.

46. Rocaboy, C.; Bauer, W.; Gladysz, J. A., Convenient Syntheses of a Family of Easily Recoverable Fluorous Primary, Secondary, and Tertiary Aliphatic Amines $\text{NH}_3\text{-x}[(\text{CH}_2)_m(\text{CF}_2)_7\text{CF}_3]_x$ ($m = 3-5$; $x = 1-3$) - Fine Tuning of Basicities and Fluorous Phase Affinities. *Eur. J. Org. Chem.* **2000**, 2621-2628.

47. Simon, W.; Wuhrmann, H. R.; Vasak, M.; Pioda, L. A. R.; Dohner, R.; Stefanac, Z., Ion-Selective Sensors. *Angew. Chem. Int. Ed.* **1970**, 9, 445-455.

48. Boswell, P. G.; Lugert, E. C.; Rábai, J.; Amin, E. A.; Bühlmann, P., Coordinative Properties of Highly Fluorinated Solvents with Amino and Ether Groups. *J. Am. Chem. Soc.* **2005**, 127, 16976-16984.

49. Anderson, E. L.; Troudt, B. K.; Bühlmann, P., Critical Comparison of Reference Electrodes with Salt Bridges Contained in Nanoporous Glass With 5, 20, 50, and 100 nm Diameter Pores. *Anal. Sci.*, published on-line 09/06/2019.

50. Meier, P. C., Two-Parameter Debye-Hückel Approximation for The Evaluation of Mean Activity-Coefficients of 109 Electrolytes. *Anal. Chim. Acta* **1982**, 136, 363-368.

51. Oesch, U.; Simon, W., Life Time of Neutral Carrier Based Ion-Selective Liquid-Membrane Electrodes. *Anal. Chem.* **1980**, 52, 692-700.

52. Ammann, D.; Pretsch, E.; Simon, W.; Lindner, E.; Bezegh, a.; Pungor, E., Lipophilic salts as membrane additives and their influence on the properties of macro- and micro-electrodes based on neutral carriers. *Anal. Chim. Acta* **1985**, 171, 119-129.

53. Jiao, H.; Le Stang, S.; Soós, T.; Meier, R.; Kowski, K.; Rademacher, P.; Jafarpour, L.; Hamard, J.-B.; Nolan, S. P.; Gladysz, J. A., How To Insulate a Reactive Site from a Perfluoroalkyl Group: Photoelectron Spectroscopy, Calorimetric, and Computational Studies of Long-Range Electronic Effects in Fluorous Phosphines $\text{P}((\text{CH}_2)_m(\text{CF}_2)_7\text{CF}_3)_3$. *J. Am. Chem. Soc.* **2002**, 124, 1516-1523.

54. Pratt, C. W., *Essential Biochemistry*. Third ed.; New York, NY, 2014.

55. Mi, Y. M.; Bakker, E., Determination of Complex Formation Constants of Lipophilic Neutral Ionophores in Solvent Polymeric Membranes with Segmented Sandwich Membranes. *Anal. Chem.* **1999**, *71*, 5279-5287.

56. Qin, Y.; Mi, Y. M.; Bakker, E., Determination of Complex Formation Constants of 18 Neutral Alkali and Alkaline Earth Metal Ionophores in Poly(Vinyl Chloride) Sensing Membranes Plasticized with Bis(2-ethylhexyl) Sebacate and o-Nitrophenyl Octyl Ether. *Anal. Chim. Acta* **2000**, *421*, 207-220.

57. Shultz, M. M.; Stefanova, O. K.; Mokrov, S. S.; Mikhelson, K. N., Potentiometric Estimation of the Stability Constants of Ion-Ionophore Complexes in Ion-Selective Membranes by the Sandwich Membrane Method: Theory, Advantages, and Limitations. *Anal. Chem.* **2002**, *74*, 510-517.

58. Bakker, E.; Willer, M.; Lerchi, M.; Seiler, K.; Pretsch, E., Determination of Complex-Formation Constants of Neutral Cation-Selective Ionophores in Solvent Polymeric Membranes. *Anal. Chem.* **1994**, *66*, 516-521.

59. Bakker, E.; Pretsch, E., Potentiometric Determination of Effective Complex Formation Constants of Lipophilic Ion Carriers within Ion-Selective Electrode Membranes. *J. Electrochem. Soc.* **1997**, *144*, L125-L127.

60. Bakker, E.; Pretsch, E., Ion-Selective Electrodes Based on Two Competitive Ionophores for Determining Effective Stability Constants of Ion-Carrier Complexes in Solvent Polymer Membranes. *Anal. Chem.* **1998**, *70*, 295-302.

61. Ceresa, A.; Pretsch, E., Determination of Formal Complex Formation Constants of Various Pb^{2+} Ionophores in the Sensor Membrane Phase. *Anal. Chim. Acta* **1999**, *395*, 41-52.

62. Kraus, C. A.; Fuoss, R. M., Properties of Electrolytic Solutions. I. Conductance as Influenced by the Dielectric Constant of the Solvent Medium. *J. Am. Chem. Soc.* **1933**, *55*, 21-36.

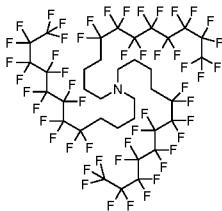
63. Anderson, E. L.; Gingery, N. M.; Boswell, P. G.; Chen, X. V.; Rábai, J.; Bühlmann, P., Ion Aggregation and $R_3N^+-C(R)-H\cdots NR_3$ Hydrogen Bonding in a Fluorous Phase. *J. Phys. Chem. B* **2016**, *120*, 11239-11246.

64. Rubinson, K. A.; Bühlmann, P.; Allison, T. C.; Krueger, S.; Moyer, J. J.; Orts, W. J.; Stevenazzi, A., One-Dimensional Ionic Self-Assembly in a Fluorous Solution: the Structure of Tetra-n-butylammonium Tetrakis 3,5-Bis(perfluorohexyl)phenyl Borate in Perfluoromethylcyclohexane by Small-Angle Neutron Scattering (SANS). *Phys. Chem. Chem. Phys.* **2016**, *18*, 9470-9475.

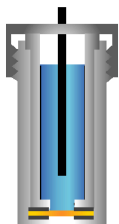
65. Yilmaz, I.; Chen, L. D.; Chen, X. V.; Anderson, E. L.; da Costa, R. C.; Gladysz, J. A.; Bühlmann, P., Potentiometric Selectivities of Ionophore-Doped Ion-Selective Membranes: Concurrent Presence of Primary Ion or Interfering Ion Complexes of Multiple Stoichiometries. *Anal. Chem.* **2019**, *91*, 2409-2417.

For Table of Contents Only

pH 2.2  11.2



Fluorophilic
Ionophore



Fluorous ISE
Membrane